Pion and Kaon box contribution to a_μ^{HLbL}

Ángel Miramontes[1,*] Adnan Bashir[1,†] Khépani Raya[2,‡] and Pablo Roig[3,§]

[1]*Instituto de Física y Matemáticas, Universidad Michoacana de San Nicolás de Hidalgo,
Morelia, Michoacán 58040, Mexico*
[2]*Departamento de Física Teórica y del Cosmos, Universidad de Granada, E-18071 Granada, Spain*
[3]*Departamento de Física, Centro de Investigación y de Estudios Avanzados del IPN,
Apartado Postal 14-740,07000 Ciudad de México, Mexico*

We present an evaluation of the $\pi^\pm$ and $K^\pm$ box contributions to the hadronic light-by-light piece of the muon's anomalous magnetic moment, a_μ. The calculation of the corresponding electromagnetic form factors (EFFs) is performed within a Dyson-Schwinger equations (DSE) approach to quantum chromodynamics. These form factors are calculated in the so-called rainbow-ladder (RL) truncation, following two different evaluation methods and, subsequently, in a further improved approximation scheme which incorporates meson cloud effects. The results are mutually consistent, indicating that in the domain of relevance for a_μ the obtained EFFs are practically equivalent. Our analysis yields the combined estimates of $a_\mu^{\pi^\pm-\text{box}} = -(15.6 \pm 0.2) \times 10^{-11}$ and $a_\mu^{K^\pm-\text{box}} = -(0.48 \pm 0.02) \times 10^{-11}$, in full agreement with results previously obtained within the DSE formalism and other contemporary estimates.

I. INTRODUCTION

There has been a renewed interest in the anomalous magnetic moment of the muon, a_μ, after the first measurement from the new muon g-2 experiment at FNAL [1]

$$a_\mu^{\text{FNAL}} = 116592040(54) \times 10^{-11}. \quad (1)$$

Combining it with the final average from the muon g-2 measurements at BNL [2] yields

$$a_\mu^{\text{Exp}} = 116592061(41) \times 10^{-11} \quad (2)$$

as the corresponding world average, which has a remarkable precision of 0.35 parts per million. On the other hand, the outcome of the Muon g-2 theory initiative for the Standard Model prediction of this quantity [3],[1]

*angel-aml@hotmail.com
†adnan.bashir@umich.mx
‡khepani@ugr.es
§proig@fis.cinvestav.mx
[1]This result is based on Refs. [4–38]. Later developments, after the cut for inclusion in the white paper [3], include Refs. [39–58].

$$a_\mu^{\text{SM}} = 116591810(43) \times 10^{-11}, \quad (3)$$

has a comparable accuracy and deviates by 4.2σ from a_μ^{exp}. This difference hints at the tantalizing prospect of new physics being at work.

The BMW lattice QCD result [59] for the dominant component of the SM uncertainty, i.e., the hadronic vacuum polarization contribution (HVP) was not taken into account for the a_μ^{SM} value in the white paper [3]. If this value were used, the incompatibility between the SM prediction and the world average is reduced to merely 1.6σ level.[2] This result needs to be confirmed or refuted by other lattice analyses achieving a similar accuracy, thus constituting a very active area of research.

The uncertainty in a_μ^{Exp} is expected to shrink further as more data is analyzed, demanding a commensurate improvement in a_μ^{SM}. Its different contributions—particularly the hadronic ones (HVP and hadronic light-by-light, HLbL), which dominate the uncertainty—are continuously refined to achieve this objective.

In this work we focus on a specific HLbL contribution to a_μ, namely, the **P**-box contributions ($\mathbf{P} = \pi^\pm, K^\pm$), depicted in Fig. 1 and denoted herein as $a_\mu^{\mathbf{P}-\text{box}}$. For pion, the dispersive evaluation of Ref. [22] achieved a considerably small uncertainty of 0.2×10^{-11}. The Dyson-Schwinger

[2]If the BMW result is adopted for a_μ^{HVP}, then there must anyway be new physics somewhere else, according to the constraints set by the electroweak precision observables [60–64].
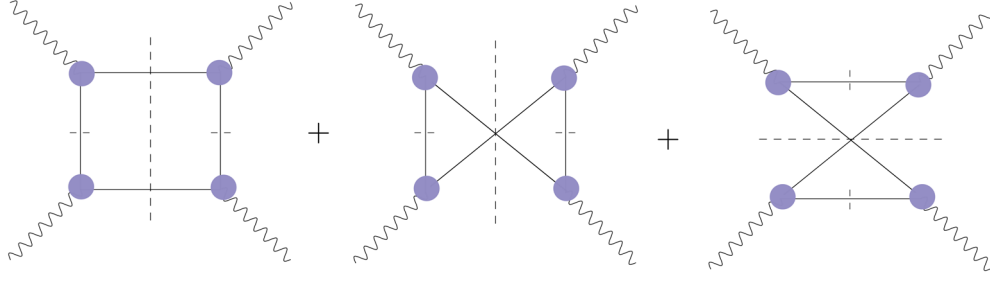
FIG. 1.   Leading order **P**-box contributions to a_μ^{HLbL}, where the corresponding **P** meson EFFs are highlighted by the purple filled circles.

equations (DSE) computation in Ref. [31] also yields a 0.02×10^{-11} overall error for the $K^\pm$ contribution. This level of accuracy serves as the reference for our corresponding computation for each case. To calculate the **P**-box contributions, we employ the master formula derived in [22], which reads:

$$a_\mu^{\mathbf{P-box}} = \frac{\alpha_{\mathrm{em}}^3}{432\pi^2} \int_\Omega \sum_i^{12} T_i(Q_1, Q_2, \tau) \bar{\Pi}_i^{\mathbf{P-box}}(Q_1, Q_2, \tau), \quad (4)$$

where α_{em} is the QED coupling constant and $\int_\Omega$ denotes the integration over the photon momenta, $Q_{1,2}$, and their relative angle τ. With $Q_3^2 = Q_1^2 + Q_2^2 + 2|Q_1||Q_2|\tau$, the functions $\bar{\Pi}_i^{\mathbf{P-box}}$ are expressed as:

$$\bar{\Pi}_i^{\mathbf{P-box}}(Q_1^2, Q_2^2, Q_3^2) = F_{\mathbf{P}}(Q_1^2) F_{\mathbf{P}}(Q_2^2) F_{\mathbf{P}}(Q_3^2)$$
$$\times \frac{1}{16\pi^2} \int_0^1 dx \int_0^{1-x} dy I_i(x, y); \quad (5)$$

the scalar functions T_i and I_i are provided in Appendices B and C, respectively, of Ref. [22]. Thus, the only missing ingredients are the electromagnetic form factors (EFFs), $F_{\mathbf{P}}(Q^2)$, obtained from the process $\gamma^* \mathbf{P} \to \mathbf{P}$.

Our approach is based upon the DSE formalism [65–67], which captures the nonperturbative character of QCD excellently well and has produced a plethora of hadron physics predictions; for instance, it unifies the description of the EFFs [31,68–71] with their corresponding distribution amplitudes and distribution functions [72–75], as well as with the $\gamma^*\gamma^* \to \{\pi^0, \eta, \eta', \eta_c, \eta_b\}$ transition form factors (TFFs) [76–80]. This manuscript is organized as follows: Sec. II describes the computation of EFFs within the DSE formalism, dissecting all the pieces entering the corresponding electromagnetic current. The numerical results of the EFFs and contributions to a_μ are presented in Sec. III. Section IV summarizes our results and conclusions.

II. ELECTROMAGNETIC FORM FACTORS IN THE DSE FORMALISM

The interaction of a virtual photon with a pseudoscalar meson is described by a single form factor, $F_{\mathbf{P}}(Q^2)$. The matrix element reads

$$\langle \mathbf{P}(p_f)|j_\mu|\mathbf{P}(p_i)\rangle = 2K_\mu F_{\mathbf{P}}(Q^2), \quad (6)$$

where $Q = p_f - p_i$ is the photon momentum and $2K = (p_f + p_i)$; the electromagnetic current is

$$j_\mu = \bar{\Gamma}_{\mathbf{P}}^f G_0(\Gamma_\mu - \mathcal{K}_\mu) G_0 \Gamma_{\mathbf{P}}^i, \quad (7)$$

with $\Gamma_{\mathbf{P}}^{i,f}$ denoting the incoming and outgoing **P** meson Bethe-Salpeter amplitudes (BSAs), respectively; G_0 represents an appropriate product of dressed quark propagators, such that

$$\Gamma_\mu = (S^{-1} \otimes S^{-1})_\mu = \Gamma_\mu \otimes S^{-1} + S^{-1} \otimes \Gamma_\mu \quad (8)$$

defines the impulse approximation (IA) [81]; this will be shown explicitly later. Beyond IA effects are encoded in $\mathcal{K}_\mu$ (see Appendix), which characterizes the interaction of the photon with the Bethe-Salpeter kernel describing the two-body interaction [68,82]. Thus, all the parts entering Eq. (6) require the knowledge of quark propagators, BSAs, quark-photon vertex (QPV), and their corresponding interaction kernels. We shall now describe how to gather those ingredients within the DSE approach.

A. Quark propagator and meson Bethe-Salpeter amplitudes

The DSEs are the QCD equations of motion, encoding full dynamics of the theory, simultaneously capturing the perturbative and nonperturbative facets of QCD [65,67]. The DSEs form an infinite set of coupled integral equations that relate the theory's Green functions; subsequently, any tractable problem demands a systematic and rigorous truncation scheme [83–86].

The DSE for the f-flavor quark propagator, also referred to as the gap equation, reads as:

$$S_f^{-1}(p) = Z_2 [S_f^{(0)}(p)]^{-1} + \int_q^\Lambda [\mathbf{K}^{(1)}(q, p)] S_f(q),$$

$$[\mathbf{K}^{(1)}(q, p)] = \frac{4}{3} Z_1 g^2 D_{\mu\nu}(p - q)[\gamma_\mu \otimes \Gamma_\nu^{fg}(p, q)], \quad (9)$$

where $\int_q^\Lambda = \int^\Lambda \frac{d^4q}{(2\pi)^4}$ stands for a Poincaré invariant regularized integration, Λ being the regularization scale.

The components that constitute the one-body kernel, $[\mathbf{K}^{(1)}]$, carry their usual meanings (color indices have been omitted for the simplicity of notation):

(i) $D_{\mu\nu}$ is the gluon propagator and g is the coupling constant for all the QCD interactions appearing in the Lagrangian.

(ii) Γ_ν^{fg} represents the fully-dressed quark-gluon vertex (QGV); in general characterized by 12 Dirac structures [87–89].

(iii) $Z_{1,2}$ are the QGV and quark wave-function renormalization constants, respectively.

Herein, $S_f^{(0)}(p) = [i\gamma \cdot p + m_f^{\mathrm{bm}}]^{-1}$ is the bare propagator and m_f^{bm} the bare fermion mass. The fully dressed quark propagator is represented as

$$S_f(p) = Z_f(p^2)(i\gamma \cdot p + M_f(p^2))^{-1}, \qquad (10)$$

in clear analogy with its bare counterpart. Multiplicative renormalization entails that the quark mass function, $M_f(p^2)$, is independent of the renormalization point ζ.

The description of mesons is obtained from the Bethe-Salpeter equation (BSE) [83–85]:

$$\Gamma_H(p; P) = \int_q^\Lambda [\mathbf{K}^{(2)}(q, p; P)]\chi_H(q; P), \qquad (11)$$

whose ingredients are defined as follows:

(i) As before, Γ_H denotes the BSA, with H labeling the type of meson.

(ii) $\chi_H(q; P) = S(q_+)\Gamma_H(q; P)S(q_-)$ corresponds to the Bethe-Salpeter wave function (BSWF).

(iii) The kinematic variables: P is the total momentum of the bound state such that $P^2 = -m_H^2$ (m_H the mass of the meson); $q_+ = q + \eta P$ and $q_- = q - (1 - \eta)P$, where $\eta \in [0, 1]$ determines the relative momentum.

The Dirac structure characterizing the BSA depends on the meson's quantum numbers. For a pseudoscalar meson **P**:

$$\Gamma_{\mathbf{P}}(q; P) = \gamma_5[i\mathbb{E}_{\mathbf{P}}(q; P) + \gamma \cdot P\mathbb{F}_{\mathbf{P}}(q; P)$$
$$+ \gamma \cdot q\mathbb{G}_{\mathbf{P}}(q; P) + q_\mu\sigma_{\mu\nu}P_\nu\mathbb{H}_{\mathbf{P}}(q; P)]. \quad (12)$$

The two-body interaction in Eq. (11) is represented by $[\mathbf{K}^{(2)}(q, p; P)]$; it corresponds to two-particle irreducible quark/antiquark scattering kernel, which contains all possible interactions between the quark and antiquark within the bound state [90]. Once the 1 and 2-body kernels have been specified (i.e., a truncation scheme has been defined), gap and Bethe-Salpeter equations can be solved. In fact, $[\mathbf{K}^{(1)}]$ and $[\mathbf{K}^{(2)}]$ are related via vector and axial-vector Ward-Green-Takahashi identities (WGTIs) [91–93], implying charge conservation and the appearance of pions and kaons (in the chiral limit) as Nambu-Goldstone bosons of dynamical chiral symmetry breaking [94].

B. Rainbow ladder truncation

The simplest truncation that fulfils vector and axial-vector WGTIs is defined by the kernel ($\{r, s, t, u\}$ are color indices):

$$[\mathbf{K}_{tu}^{rs}]^{\mathrm{RL}}(q, p; P) = -\frac{4}{3}Z_2^2 D_{\mu\nu}^{\mathrm{eff}}(p - q)[\gamma_\mu]_{ts} \otimes [\gamma_\nu]_{ru}, \quad (13)$$

which relate the 1-body and 2-body kernels as:

$$\mathbf{K}^{(2)}(q, p; P) = \mathbf{K}^{\mathrm{RL}}(q, p; P) = -\mathbf{K}^{(1)}(q, p; P). \quad (14)$$

This truncation is dubbed as the RL truncation [94]. It provides a reliable and practical approach so long as we restrain ourselves to ground-state pseudoscalar and vector mesons [71,72,76,95]. It is worth noticing that the gluon propagator has been demoted to an effective one, $gD_{\mu\nu} \to D_{\mu\nu}^{\mathrm{eff}}$, where:

$$D_{\mu\nu}^{\mathrm{eff}}(k) = \left(\delta_{\mu\nu} - \frac{k_\mu k_\nu}{k^2}\right)\mathcal{G}(k^2). \quad (15)$$

Herein, $\mathcal{G}(k^2)$ is an effective coupling, typically obtained from either lattice QCD or phenomenological models [96–98]. Throughout this work, we shall employ the well-known Qin-Chang (QC) interaction [98]:

$$\mathcal{G}(q^2) = \frac{8\pi^2}{\omega^4}De^{-\frac{q^2}{\omega^2}} + \frac{2\pi\gamma_m(1 - e^{-q^2/\Lambda_t^2})}{\ln[e^2 - 1 + (1 + q^2/\Lambda_{\mathrm{QCD}}^2)^2]}. \quad (16)$$

The first term above controls the strength of the effective coupling, in such a way that the QC model is defined once the mass parameter, $m_G = (wD)^{1/3}$, is fixed to produce the masses and decay constants of the ground-state pseudoscalar mesons. Typical RL parameters are $m_G \sim 0.8$ GeV and $w \sim 0.5$ GeV; herein, the later is varied within the range $w \in (0.4, 0.6)$ to estimate model uncertainties. The second term is simply set to reproduce the 1-loop behavior of the QCD's running coupling: $\gamma_m = 12/(11N_C - 2N_f) = 12/25$ is the anomalous dimension, with $N_f = 4$ flavors and $N_c = 3$ colors, and $\Lambda_{\mathrm{QCD}} = 0.234$ GeV; the parameter $\Lambda_t = 1$ GeV is introduced for technical reasons and has no material impact on the computed observables. Table I collects the RL inputs and some static properties of the pion and kaon.

It is worth mentioning that the RL truncation is self-consistent with the IA, in such a way that the EFF is obtained from:

$$2K_\mu F_{\mathbf{P}}(Q^2) = e_u[F_{\mathbf{P}}^u(Q^2)]_\mu + e_{\bar{h}}[F_{\mathbf{P}}^{\bar{h}}(Q^2)]_\mu, \quad (17)$$

where **P** is a $u\bar{h}$ meson and $e_{u,\bar{h}}$ are the electric charges of the quark and antiquark, respectively. $[F_{\mathbf{P}}^f(Q^2)]_\mu$ denotes

TABLE I.   RL and BRL parameters ($m_u = m_d$, m_s and m_G), fixed to produce the ground-state masses and decay constants (quoted in GeV). Physical observables exhibit mild sensitivity to the variation of $w^{\text{RL}} \in (0.4, 0.6)$ GeV and $w^{\text{BRL}} \in (0.6, 0.8)$ GeV; this variation, however, is taken into account for the calculation of the electromagnetic form factors. Charge radii (in fm) are obtained from Eq. (24).

	m_u	m_s	m_G	m_π	f_π	r_π	m_k	f_k	r_k
RL	0.0052	0.122	0.80	0.139 (3)	0.131 (2)	0.677 (4)	0.493 (4)	0.157 (2)	0.597 (3)
BRL	0.0060	0.125	0.84	0.139 (4)	0.131 (2)	0.676 (2)	0.493 (5)	0.159 (2)	0.593 (2)

the interaction of the photon with a valence constituent f-in-**P**, such that:

$$[F_{\mathbf{P}}^f(Q^2)]_\mu = \text{tr}_{CD} \int_q \chi_\mu^f(q + p_f, q + p_i)$$
$$\times \Gamma_{\mathbf{P}}(q_i; p_i) S(q) \Gamma_{\mathbf{P}}(q_f; -p_f). \quad (18)$$

The kinematics is defined as follows: $p_{i,f} = K \mp Q/2$ and $q_{i,f} = q + p_{i,f}/2$, such that $p_{i,f}^2 = -m_{\mathbf{P}}^2$; naturally, $m_{\mathbf{P}}$ is the mass of the pseudoscalar meson and Q the photon momentum. The trace, tr_{CD}, is taken over color and Dirac indices. The only remaining ingredient to compute the EFFs in the RL approximation is the QPV. This is described below.

C. Quark-photon vertex

The QPV might be obtained via the inhomogeneous BSE:

$$\Gamma_\mu^f(p; P) = \gamma_\mu + \int_q^\Lambda [\mathbf{K}^{(2)}(q, p; P)] \chi_\mu^f(q; P), \quad (19)$$

where $\chi_\mu^f(q; P)$ is simply the unamputated vertex,

$$\chi_\mu^f(q; P) = S^f(q_+) \Gamma_\mu^f(q; P) S^f(q_-). \quad (20)$$

The choice of the 2-body kernel in Eq. (19) renders the QPV self-consistent with the chosen truncation, ensuring, for example, that the Abelian anomaly related with the process $\gamma\gamma \to \pi^0$ is faithfully reproduced [99,100]. For the purpose of clarity, we refer to this approach as the direct computation.

In the RL truncation, vector meson bound states appear as poles on the negative real axis in the Q^2 plane in the inhomogeneous BSE for the QPV [101] and, as a consequence, in the timelike form factors. The appropriate inclusion of these poles favors obtaining the correct value for the charge radius [81,101]. The EFFs in the timelike region are harder to describe in the DSE-BSE approach. For all practical purposes, this should not affect the way EFFs contribute to a_μ, because only a relatively small spacelike region of the corresponding form factors near $Q^2 = 0$ actually matters for determining their contribution [31,79]. We expect this small effect to be virtually remedied

by adjusting the model parameters to reproduce the correct value of the charge radius.

Notwithstanding, it is worth exploring and reassuring our expectations through a proper treatment of the timelike region. In order to shift the vector meson poles appearing in the QPV to the complex plane, and turn the bound state into a resonance with a nonvanishing decay width, the interaction kernels $\mathbf{K}^{(1,2)}$ must allow virtual decays into suitable channels [102,103]. The truncation explored in [82] and employed in [68] for the calculation of the pion timelike EFF, denoted herein as *beyond rainbow-ladder* (BRL), takes into account resonance effects and incorporates meson cloud effects (MCEs) in the description of the pion EFF. This is sufficient to produce the correct behavior of the pion EFF in the timelike axis. We adapt this approach to compute the $\pi - K$ EFFs and corresponding box contributions. As Eq. (7) suggests, it is also desirable to go beyond the IA. Nevertheless, to alleviate the numerical calculations we neglect further photon couplings and consider the IA only. Some aspects of the calculation of EFFs in the BRL truncation are canvassed herein, in Appendix, and detailed through Refs. [68,82]. As clarified in Table I, the QC model favors $m_G = 0.87$ GeV and $\omega \sim 0.7$ GeV.

Due to technical reasons, when employing the QPV obtained from Eq. (19), the calculation of EFF is limited to a certain domain of spacelike momenta. For instance, the pion elastic and $\gamma^*\gamma \to \pi^0$ transition form factors can only be obtained up to $Q^2 \sim 4$ GeV^2 [81,100], without appealing to sophisticated mathematical techniques for extrapolation [80]. While not the entire spacelike domain is crucial to a_μ, it is reassuring to access it in its entirety.[3] For this reason and in direct connection with our previous work on the HLbL contributions of neutral pseudoscalars [79], we also present an alternative technique, based upon perturbation theory integral representations (PTIRs), to evaluate the form factors at arbitrarily large momenta.

D. The PTIR approach

A practical PTIR approach for the quark propagators and BSAs was put forward in [71,75], to calculate the pion distribution amplitude and spacelike EFF. It was subsequently implemented to the case of $\gamma^*\gamma^*$ TFFs [76–79].

---

[3]The large-Q^2 behavior of the $\gamma^*\gamma^*$ TFFs is quite useful to parametrize the numerical solutions [79,104].

The general idea, which applies to all pseudoscalars, is to describe the quark propagators in terms of $j_m = 2$ complex conjugate poles (CCPs), and express the BSAs, $\mathcal{A}_j$, as follows:

$$\mathcal{A}_j(k;P) = \sum_{i=1}^{i_n} \int_{-1}^{1} dw \rho_i^j(w) \frac{c_i^j (\Lambda_{i,j}^2)^{\beta_i^j}}{(k^2 + wk \cdot P + \Lambda_{i,j}^2)^{\alpha_i^j}}. \quad (21a)$$

The interpolation parameters involved, i.e., $\{z_j, m_j\}$, $\{\alpha_i^j, \beta_i^j, \Lambda_{i,j}, c_i^j, i_n = 3\}$ (for quark propagators and BSAs, respectively), as well as the spectral weights, $\rho_i^j(w)$, are determined through fitting of the numerical results of the corresponding DSE-BSEs. The carefully constructed sets of RL truncation parameters are found in Refs. [74,76].

Constructing a PTIR for the QPV in Eq. (19) turns out to be difficult and unpractical [95]. Thus, appealing to gauge covariance properties [105], the following Ansatz has been proposed and systematically tested [76–79]:

$$\chi_\mu^f(k_o, k_i) = \gamma_\mu \Delta_{k^2 \sigma_V}^f$$

$$+ [\mathbf{s}_f \gamma \cdot k_o \gamma_\mu \gamma \cdot k_i + \bar{\mathbf{s}}_f \gamma \cdot k_i \gamma_\mu \gamma \cdot k_o] \Delta_{\sigma_V}^f$$

$$+ [\mathbf{s}_f (\gamma \cdot k_o \gamma_\mu + \gamma_\mu \gamma \cdot k_i)$$

$$+ \bar{\mathbf{s}} (\gamma \cdot k_i \gamma_\mu + \gamma_\mu \gamma \cdot k_o)] i \Delta_{\sigma_S}^f, \quad (22)$$

where $\Delta_\phi^f = [\phi^f(k_o^2) - \phi^f(k_i^2)]/(k_o^2 - k_i^2)$ and $\bar{\mathbf{s}}_f = 1 - \mathbf{s}_f$. According to [79], the transverse pieces are weighted by

$$\mathbf{s}_f = \mathbf{s}_f \exp\left[-\left(\sqrt{Q_1^2/4 + m_P^2} - m_P\right)/M_f^E\right], \quad (23)$$

such that the strength parameter $\mathbf{s}_f$ is tuned to reproduce the π^0 Abelian anomaly and $\gamma\gamma \to \{\eta, \eta', \eta_c\}$ empirical decay widths. Nonetheless, as confirmed by our numerical evaluations, such weighting for the case of the EFFs is irrelevant and one can simply set $\mathbf{s}_f$ to zero. The reasons can be easily understood: first, the terms which dominate at low-Q^2 in Eq. (18), those involving the product of leading BSAs ($\mathbb{E}_P \times \mathbb{E}_P$), are not affected at all by the choice of $\mathbf{s}_f$ since the corresponding trace is exactly zero; then, with $F_P(Q^2 = 0) = 1$ entirely fixed by charge conservation, being exponentially suppressed, the $\mathbf{s}_f$-weighted subleading terms could only provide a minor contribution in neighborhood of $Q^2 \sim 0$.

Defined as in Eq. (22), the QPV is fully written in terms of the quark propagator dressing functions.[4] With all the ingredients in Eqs. (17) and (18) expressed in a PTIR, the evaluation of the 4-momentum integral follows after a series of standard algebraic steps (numerical integration is only carried out for the Feynman parameters and spectral

---

[4] The f-quark propagator expressed $S_f(p) = -i\gamma \cdot p \sigma_v^f(p^2) + \sigma_s^f(p^2)$, with $\sigma_{s,v}^f(p^2)$ being algebraically related to $M_f(p^2)$ and $Z_f(p^2)$ in Eq. (10).

weights). Hence, the form factors can be calculated at arbitrarily large spacelike momenta.

III. NUMERICAL RESULTS

A. Electromagnetic form factors

The $\pi - K$ EFFs are presented in Fig. 2. We compare the RL results which follow from the direct computation and PTIR approach; the compatibility between both calculations is evident. In the domain of interest, the BRL truncation yields similar outcomes. Furthermore, our obtained EFFs are in clear agreement with the DSE results reported in Ref. [31]. The charge radii are obtained from the derivative of the form factor:

$$r_P^2 = -6 \frac{dF_P(Q^2)}{dQ^2}\bigg|_{Q^2=0}. \quad (24)$$

Both RL and BRL direct computations yield similar values: $r_\pi = 0.677(4)$ fm and $r_K = 0.597(3)$ fm (RL), and
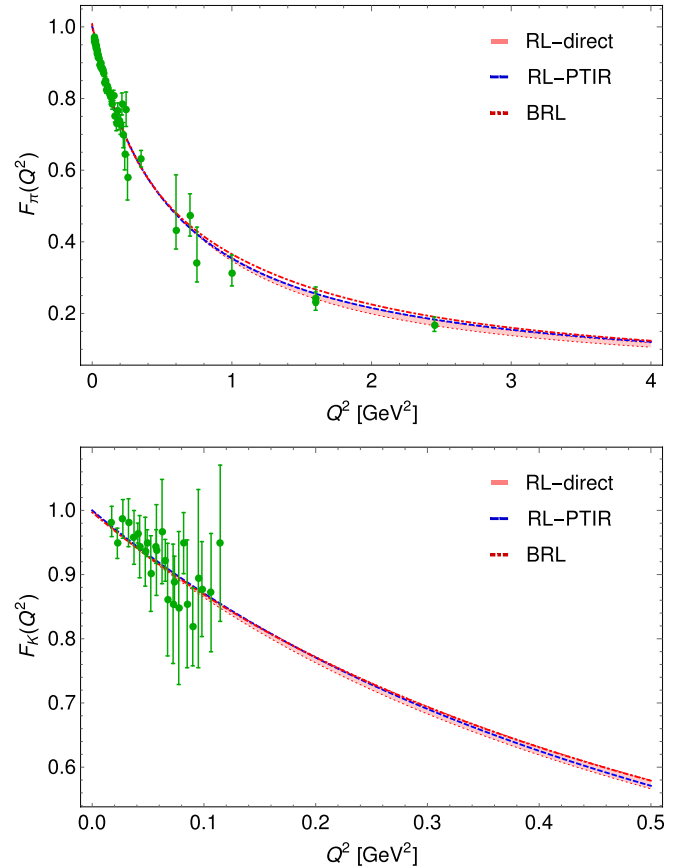

FIG. 2. π^+ and K^+ EFFs. The narrow band in the RL-direct result accounts for the variation of the QC model parameters, as described in text; those corresponding to the PTIR and BRL results are not shown, since there is a considerable overlap. The charge radii, Table I, are practically insensitive to the model inputs and truncation. Experimental data is taken from Refs. [106–109].

$r_\pi = 0.676(2)$ fm and $r_K = 0.593(2)$ fm (BRL); the error accounts for the variation of ω in the QC model, as explained in Table I. The RL-PTIR case also falls within these values: $r_\pi = 0.676(5)$ fm and $r_K = 0.596(5)$.

B. Pion and kaon box contributions

The integrations in Eqs. (4)–(5) have been carried out employing the CUBA library [110], benchmarked with the vector meson dominance (VMD) ansätze of the form factors:

$$F_{\pi^+}^{\text{VMD}}(Q^2) = \frac{m_\rho^2}{m_\rho^2 + Q^2}, \tag{25}$$

$$F_{K^+}^{\text{VMD}}(Q^2) = 1 - \frac{Q^2}{2}\left[\frac{1}{m_\rho^2 + Q^2} + \frac{1}{3}\left(\frac{1}{m_\omega^2 + Q^2}\right)\right.$$
$$\left. + \frac{2}{3}\left(\frac{1}{m_\phi^2 + Q^2}\right)\right], \tag{26}$$

which yield the results

$$a_\mu^{\pi^\pm-\text{box}} = -16.4 \times 10^{-11} \quad [\text{RL-PTIR}],$$
$$a_\mu^{K^\pm-\text{box}} = -0.5 \times 10^{-11} \quad [\text{BRL}], \tag{27}$$

where we have employed $m_\pi = 0.13957$ GeV, $m_K = 0.49367$ GeV, $m_\rho = 0.7752$ GeV, $m_\omega = 0.7827$ GeV, $m_\phi = 1.0195$ GeV, $m_\mu = 0.10565$ GeV and $\alpha_{\text{em}} = 1/137.03599$ [111]. The estimates in Eq. (27) match those quoted in [31], and the integration errors have been omitted, since those are two orders of magnitude smaller.

With the EFFs obtained in the RL (direct and PTIR) and BRL truncations, the numerical estimates for the $\pi^\pm -$ box contributions are

$$a_\mu^{\pi^\pm-\text{box}} = -(15.4 \pm 0.3) \times 10^{-11} \quad [\text{RL-direct}],$$
$$a_\mu^{\pi^\pm-\text{box}} = -(15.6 \pm 0.3) \times 10^{-11} \quad [\text{RL-PTIR}],$$
$$a_\mu^{\pi^\pm-\text{box}} = -(15.7 \pm 0.2) \times 10^{-11} \quad [\text{BRL}]. \tag{28}$$

Analogous results for the $K^\pm$ case yield:

$$a_\mu^{K^\pm-\text{box}} = -(0.47 \pm 0.03) \times 10^{-11} \quad [\text{RL-direct}],$$
$$a_\mu^{K^\pm-\text{box}} = -(0.48 \pm 0.03) \times 10^{-11} \quad [\text{RL-PTIR}],$$
$$a_\mu^{K^\pm-\text{box}} = -(0.48 \pm 0.02) \times 10^{-11} \quad [\text{BRL}]. \tag{29}$$

From Fig. 2 and the above estimates, it is clear that the direct and PTIR approach are virtually indistinguishable; the BRL truncation also yields similar outcomes. Therefore, one can combine the estimates in Eqs. (28)–(29) to produce:

$$a_\mu^{\pi^\pm-\text{box}} = -(15.6 \pm 0.2) \times 10^{-11}, \tag{30}$$

$$a_\mu^{K^\pm-\text{box}} = -(0.48 \pm 0.02) \times 10^{-11}, \tag{31}$$

where the weighted errors have been added.

Our result for the $\pi^\pm$-box contribution agrees remarkably with the dispersive one, $-15.9(2) \times 10^{-11}$ [22] and an earlier DSE evaluation, $-15.7(2)(3) \times 10^{-11}$ [31] (see also Ref. [99]). In the case of the $K^\pm$-box contribution, we agree again with the previous DSE computation [31], $-0.48(2)(4) \times 10^{-11}$, which yields $-0.46(2) \times 10^{-11}$ once the integration error is improved [3]. We note that the K^0-box contribution is very much suppressed, as can be seen from its VMD description in the ideal ω-ϕ mixing case

$$F_{K^0}^{\text{VMD}}(Q^2) = \frac{Q^2}{2}\left[-\frac{1}{m_\rho^2 + Q^2} + \frac{1}{3}\left(\frac{2}{m_\omega^2 + Q^2}\right)\right.$$
$$\left. + \frac{2}{3}\left(\frac{1}{m_\phi^2 + Q^2}\right)\right], \tag{32}$$

which yields the negligible result $\sim 1 \times 10^{-15}$ [3]. Consequently, we do not evaluate this contribution in our framework.

IV. CONCLUSIONS AND SCOPE

We describe the computation of the EFFs $\gamma^* \mathbf{P} \to \mathbf{P}$ within the DSE approach to QCD, leading to the evaluation of their contributions to a_μ. The EFFs were obtained, firstly, in the RL truncation. Direct computations and the PTIR approach were shown to be fully compatible, while also being in agreement with the DSE results from Refs. [31,99]. Our previous calculation of the ground-state pseudoscalar pole contributions reinforces this finding [79]. It was confirmed that the BRL truncation, which incorporates meson cloud effects, [5] produces similar EFFs in the relevant domain for a_μ; the value of the latter being barely affected by the new effects in the truncation.

In this way, we have highlighted how the DSE formalism is a robust approach for calculations of hadronic observables, including quantities of interest for the muon $g - 2$. We hope to continue developing calculations related to the subject; for instance, the importance of axial mesons has been discussed in [32], and the contribution coming from excited states might be relevant as well.

---

[5]For spacelike EFFs, meson cloud effects take place in the neighborhood of $Q^2 \approx 0$ [112–114], such that, for increasing Q^2, BRL $\to$ RL.

APPENDIX: BEYOND RAINBOW-LADDER TRUNCATION

In the RL truncation, the meson bound states appear as poles on the negative real axis on the Q^2 plane in the inhomogeneous BSE for the quark-photon vertex and, as a consequence, in the calculation of form factors in the timelike regime. In order to move the pole from the real axis to the complex plane and turn the bound state into a resonance state with a nonvanishing decay width, the interaction kernel K must allow virtual decays into suitable channels. In Refs. [102,103], pion cloud effects were investigated by the inclusion of pionic degrees of freedom in the quark propagator DSE and in the BSE interaction kernel. In such BRL truncation the quark propagator is modified by ($k = p - q$ and $\bar{k} = (p + q)/2$):

$$
S_f^{-1}(p) = S_f^{-1}(p)^{\text{RL}} - \frac{3}{2} Z_2 \int_q^{\Lambda} [\gamma_5 S(q) \Gamma_{\mathbf{P}}(\bar{k}, -k)
$$

$$
+ \gamma_5 S(q) \Gamma_{\mathbf{P}}(\bar{k}, k)] \frac{D_{\mathbf{P}}(k)}{2}, \tag{A1}
$$

with $S^{-1}(p)^{\text{RL}}$ being the right-hand side of Eq. (9) in the RL truncation, Eqs. (13), (14), and $D_{\mathbf{P}}(k) = (k^2 + m_{\mathbf{P}}^2)^{-1}$. The quark propagator in Eq. (A1) preserves the axial-vector WGTI identity in combination with the following interaction kernel for the $t-$ channel pseudoscalar exchange [68,82]:

$$
\mathbf{K}_{sr}^{tu}(q, p; P) = -\frac{3}{16} ([\Gamma_{\mathbf{P}}^j]_{ru}(\bar{k} - P/2; k)[Z_2 \tau^j \gamma^5]_{ts}
$$

$$
+ [\Gamma_{\mathbf{P}}^j]_{ru}(\bar{k} - P/2; -k)[Z_2 \tau^j \gamma^5]_{ts}
$$

$$
+ [\Gamma_{\mathbf{P}}^j]_{ts}(\bar{k} - P/2; k)[Z_2 \tau^j \gamma^5]_{ru}
$$

$$
+ [\Gamma_{\mathbf{P}}^j]_{ts}(\bar{k} - P/2; -k)[Z_2 \tau^j \gamma^5]_{ru}) D_{\mathbf{P}}(k).
$$

Analogous expressions for the s and u channels might be found in [82]; beyond IA corrections to Eq. (7), $\mathcal{K}_\mu$ are given in [68].

[1] B. Abi *et al.*, Measurement of the Positive Muon Anomalous Magnetic Moment to 0.46 ppm, Phys. Rev. Lett. **126,** 141801 (2021).

[2] G. W. Bennett *et al.*, Final report of the muon E821 anomalous magnetic moment measurement at BNL, Phys. Rev. D **73,** 072003 (2006).

[3] T. Aoyama *et al.*, The anomalous magnetic moment of the muon in the Standard Model, Phys. Rep. **887,** 1 (2020).

[4] Michel Davier, Andreas Hoecker, Bogdan Malaescu, and Zhiqing Zhang, Reevaluation of the hadronic vacuum polarisation contributions to the Standard Model predictions of the muon $g - 2$ and $\alpha(m_Z^2)$ using newest hadronic cross-section data, Eur. Phys. J. C **77,** 827 (2017).

[5] Alexander Keshavarzi, Daisuke Nomura, and Thomas Teubner, Muon $g - 2$ and $\alpha(M_Z^2)$: A new data-based analysis, Phys. Rev. D **97,** 114025 (2018).

[6] Gilberto Colangelo, Martin Hoferichter, and Peter Stoffer, Two-pion contribution to hadronic vacuum polarization, J. High Energy Phys. 02 (**2019**) 006.

[7] Martin Hoferichter, Bai-Long Hoid, and Bastian Kubis, Three-pion contribution to hadronic vacuum polarization, J. High Energy Phys. 08 (2019) 137.

[8] M. Davier, A. Hoecker, B. Malaescu, and Z. Zhang, A new evaluation of the hadronic vacuum polarisation contributions to the muon anomalous magnetic moment and to $\alpha(\mathbf{m_Z^2})$, Eur. Phys. J. C **80,** 241 (2020); Erratum, Eur. Phys. J. C **80,** 410 (2020).

[9] Alexander Keshavarzi, Daisuke Nomura, and Thomas Teubner, $g - 2$ of charged leptons, $\alpha(M_Z^2)$, and the hyperfine splitting of muonium, Phys. Rev. D **101,** 014029 (2020).

[10] Alexander Kurz, Tao Liu, Peter Marquard, and Matthias Steinhauser, Hadronic contribution to the muon anomalous magnetic moment to next-to-next-to-leading order, Phys. Lett. B **734,** 144 (2014).

[11] B. Chakraborty *et al.*, Strong-Isospin-Breaking Correction to the Muon Anomalous Magnetic Moment from Lattice QCD at the Physical Point, Phys. Rev. Lett. **120,** 152001 (2018).

[12] Sz. Borsanyi *et al.*, Hadronic Vacuum Polarization Contribution to the Anomalous Magnetic Moments of Leptons from First Principles, Phys. Rev. Lett. **121,** 022002 (2018).

[13] T. Blum, P. A. Boyle, V. Gülpers, T. Izubuchi, L. Jin, C. Jung, A. Jüttner, C. Lehner, A. Portelli, and J. T. Tsang, Calculation of the Hadronic Vacuum Polarization Contribution to the Muon Anomalous Magnetic Moment, Phys. Rev. Lett. **121,** 022003 (2018).

[14] D. Giusti, V. Lubicz, G. Martinelli, F. Sanfilippo, and S. Simula, Electromagnetic and strong isospin-breaking corrections to the muon $g - 2$ from Lattice QCD + QED, Phys. Rev. D **99,** 114502 (2019).

[15] Eigo Shintani and Yoshinobu Kuramashi, Hadronic vacuum polarization contribution to the muon $g - 2$ with $2 + 1$ flavor lattice QCD on a larger than $(10 \text{ fm})^4$ lattice at the physical point, Phys. Rev. D **100,** 034517 (2019).

[16] C. T. H. Davies *et al.*, Hadronic-vacuum-polarization contribution to the muon's anomalous magnetic moment from four-flavor lattice QCD, Phys. Rev. D **101,** 034512 (2020).

[17] Antoine Gérardin, Marco Cè, Georg von Hippel, Ben Hörz, Harvey B. Meyer, Daniel Mohler, Konstantin Ottnad, Jonas Wilhelm, and Hartmut Wittig, The leading hadronic contribution to $(g-2)_\mu$ from lattice QCD with $N_f = 2 + 1$ flavours of $O(a)$ improved Wilson quarks, Phys. Rev. D **100,** 014510 (2019).

[18] Christopher Aubin, Thomas Blum, Cheng Tu, Maarten Golterman, Chulwoo Jung, and Santiago Peris, Light quark vacuum polarization at the physical point and contribution to the muon $g-2$, Phys. Rev. D **101,** 014503 (2020).

[19] D. Giusti and S. Simula, Lepton anomalous magnetic moments in Lattice QCD + QED, Proc. Sci., LATTICE2019 (**2019**) 104.

[20] Kirill Melnikov and Arkady Vainshtein, Hadronic light-by-light scattering contribution to the muon anomalous magnetic moment revisited, Phys. Rev. D **70,** 113006 (2004).

[21] Pere Masjuan and Pablo Sanchez-Puertas, Pseudoscalar-pole contribution to the $(g_\mu - 2)$: A rational approach, Phys. Rev. D **95,** 054026 (2017).

[22] Gilberto Colangelo, Martin Hoferichter, Massimiliano Procura, and Peter Stoffer, Dispersion relation for hadronic light-by-light scattering: Two-pion contributions, J. High Energy Phys. 04 (2017) 161.

[23] Martin Hoferichter, Bai-Long Hoid, Bastian Kubis, Stefan Leupold, and Sebastian P. Schneider, Dispersion relation for hadronic light-by-light scattering: pion pole, J. High Energy Phys. 10 (2018) 141.

[24] Antoine Gérardin, Harvey B. Meyer, and Andreas Nyffeler, Lattice calculation of the pion transition form factor with $N_f = 2 + 1$ Wilson quarks, Phys. Rev. D **100,** 034520 (2019).

[25] Johan Bijnens, Nils Hermansson-Truedsson, and Antonio Rodríguez-Sánchez, Short-distance constraints for the HLbL contribution to the muon anomalous magnetic moment, Phys. Lett. B **798,** 134994 (2019).

[26] Gilberto Colangelo, Franziska Hagelstein, Martin Hoferichter, Laetitia Laub, and Peter Stoffer, Longitudinal short-distance constraints for the hadronic light-by-light contribution to $(g-2)_\mu$ with large-N_c Regge models, J. High Energy Phys. 03 (**2020**) 101.

[27] Vladyslav Pauk and Marc Vanderhaeghen, Single meson contributions to the muon's anomalous magnetic moment, Eur. Phys. J. C **74,** 3008 (2014).

[28] Igor Danilkin and Marc Vanderhaeghen, Light-by-light scattering sum rules in light of new data, Phys. Rev. D **95,** 014019 (2017).

[29] Friedrich Jegerlehner, *The Anomalous Magnetic Moment of the Muon*, Vol. 274 (Springer, Cham, 2017).

[30] M. Knecht, S. Narison, A. Rabemananjara, and D. Rabetiarivony, Scalar meson contributions to a μ from hadronic light-by-light scattering, Phys. Lett. B **787,** 111 (2018).

[31] Gernot Eichmann, Christian S. Fischer, and Richard Williams, Kaon-box contribution to the anomalous magnetic moment of the muon, Phys. Rev. D **101,** 054015 (2020).

[32] Pablo Roig and Pablo Sanchez-Puertas, Axial-vector exchange contribution to the hadronic light-by-light piece of the muon anomalous magnetic moment, Phys. Rev. D **101,** 074019 (2020).

[33] Gilberto Colangelo, Martin Hoferichter, Andreas Nyffeler, Massimo Passera, and Peter Stoffer, Remarks on higher-order hadronic corrections to the muon $g-2$, Phys. Lett. B **735,** 90 (2014).

[34] Thomas Blum, Norman Christ, Masashi Hayakawa, Taku Izubuchi, Luchang Jin, Chulwoo Jung, and Christoph Lehner, Hadronic Light-by-Light Scattering Contribution to the Muon Anomalous Magnetic Moment from Lattice QCD, Phys. Rev. Lett. **124,** 132002 (2020).

[35] Tatsumi Aoyama, Masashi Hayakawa, Toichiro Kinoshita, and Makiko Nio, Complete Tenth-Order QED Contribution to the Muon g-2, Phys. Rev. Lett. **109,** 111808 (2012).

[36] Tatsumi Aoyama, Toichiro Kinoshita, and Makiko Nio, Theory of the anomalous magnetic moment of the electron, Atoms **7,** 28 (2019).

[37] Andrzej Czarnecki, William J. Marciano, and Arkady Vainshtein, Refinements in electroweak contributions to the muon anomalous magnetic moment, Phys. Rev. D **67,** 073006 (2003); Erratum, Phys. Rev. D **73,** 119901 (2006).

[38] C. Gnendiger, D. Stöckinger, and H. Stöckinger-Kim, The electroweak contributions to $(g-2)_\mu$ after the Higgs boson mass measurement, Phys. Rev. D **88,** 053005 (2013).

[39] D. Giusti and S. Simula, Ratios of the hadronic contributions to the lepton $g-2$ from Lattice QCD + QED simulations, Phys. Rev. D **102,** 054503 (2020).

[40] Marc Knecht, On some short-distance properties of the fourth-rank hadronic vacuum polarization tensor and the anomalous magnetic moment of the muon, J. High Energy Phys. 08 (2020) 056.

[41] Pere Masjuan, Pablo Roig, and Pablo Sanchez-Puertas, The interplay of transverse degrees of freedom and axial-vector mesons with short-distance constraints in $g-2$, J. Phys. G **49,** 015002 (2022).

[42] Jan Lüdtke and Massimiliano Procura, Effects of longitudinal short-distance constraints on the hadronic light-by-light contribution to the muon **g** − **2**, Eur. Phys. J. C **80,** 1108 (2020).

[43] J. A. Miranda and P. Roig, New τ-based evaluation of the hadronic contribution to the vacuum polarization piece of the muon anomalous magnetic moment, Phys. Rev. D **102,** 114017 (2020).

[44] Bai-Long Hoid, Martin Hoferichter, and Bastian Kubis, Hadronic vacuum polarization and vector-meson resonance parameters from $e^+ e^- \to \pi^0 \gamma$, Eur. Phys. J. C **80,** 988 (2020).

[45] B. Ananthanarayan, Irinel Caprini, and Diganta Das, Test of analyticity and unitarity for the pion form-factor data around the ρ resonance, Phys. Rev. D **102,** 096003 (2020).

[46] Christopher Aubin, Thomas Blum, Maarten Golterman, and Santiago Peris, Application of effective field theory to finite-volume effects in a_μ^{HVP}, Phys. Rev. D **102,** 094511 (2020).

[47] Johan Bijnens, Nils Hermansson-Truedsson, Laetitia Laub, and Antonio Rodríguez-Sánchez, Short-distance HLbL contributions to the muon anomalous magnetic moment beyond perturbation theory, J. High Energy Phys. 10 (2020) 203.

[48] Wen Qin, Ling-Yun Dai, and Jorge Portoles, Two and three pseudoscalar production in e$^+$e annihilation and their contributions to $(g-2)_\mu$, J. High Energy Phys. 03 (2021) 092.

[49] Johan Bijnens, Nils Hermansson-Truedsson, Laetitia Laub, and Antonio Rodríguez-Sánchez, The two-loop perturbative correction to the $(g2)_\mu$ HLbL at short distances, J. High Energy Phys. 04 (**2021**) 240.

[50] Marvin Zanke, Martin Hoferichter, and Bastian Kubis, On the transition form factors of the axial-vector resonance $f_1(1285)$ and its decay into e^+e^-, J. High Energy Phys. 07 (2021) 106.

[51] En-Hung Chao, Renwick J. Hudspith, Antoine Gérardin, Jeremy R. Green, Harvey B. Meyer, and Konstantin Ottnad, Hadronic light-by-light contribution to $(g-2)_\mu$ from lattice QCD: A complete calculation, Eur. Phys. J. C **81,** 651 (2021).

[52] Igor Danilkin, Martin Hoferichter, and Peter Stoffer, A dispersive estimate of scalar contributions to hadronic light-by-light scattering, Phys. Lett. B **820,** 136502 (2021).

[53] Gilberto Colangelo, Franziska Hagelstein, Martin Hoferichter, Laetitia Laub, and Peter Stoffer, Short-distance constraints for the longitudinal component of the hadronic light-by-light amplitude: An update, Eur. Phys. J. C **81,** 702 (2021).

[54] Jing-Yu Yi, Zhong-Yu Wang, and C. W. Xiao, Study of the pion vector form factor and its contribution to the muon $g-2$, Phys. Rev. D **104,** 116017 (2021).

[55] Josef Leutgeb and Anton Rebhan, Hadronic light-by-light contribution to the muon g-2 from holographic QCD with massive pions, Phys. Rev. D **104,** 094017 (2021).

[56] Christopher L. James, Randy Lewis, and Kim Maltman, A ChPT estimate of the strong-isospin-breaking contribution to the anomalous magnetic moment of the muon, arXiv:2109.13729.

[57] Gilberto Colangelo, Martin Hoferichter, Bastian Kubis, Malwin Niehus, and Jacobo Ruiz de Elvira, Chiral extrapolation of hadronic vacuum polarization, Phys. Lett. B **825,** 136852 (2022).

[58] Martin Hoferichter and Thomas Teubner, Mixed Leptonic and Hadronic Corrections to the Anomalous Magnetic Moment of the Muon, Phys. Rev. Lett. **128,** 112002 (2022).

[59] Sz. Borsanyi *et al.*, Leading hadronic contribution to the muon magnetic moment from lattice QCD, Nature (London) **593,** 51 (2021).

[60] Andreas Crivellin, Martin Hoferichter, Claudio Andrea Manzari, and Marc Montull, Hadronic Vacuum Polarization: $(g-2)_\mu$ versus Global Electroweak Fits, Phys. Rev. Lett. **125,** 091801 (2020).

[61] Alexander Keshavarzi, William J. Marciano, Massimo Passera, and Alberto Sirlin, Muon $g-2$ and $\Delta\alpha$ connection, Phys. Rev. D **102,** 033002 (2020).

[62] Eduardo de Rafael, Constraints between $\Delta\alpha_{\text{had}}(M_Z^2)$ and $(g_\mu-2)_{\text{HVP}}$, Phys. Rev. D **102,** 056025 (2020).

[63] Bogdan Malaescu and Matthias Schott, Impact of correlations between a_μ and α_{QED} on the EW fit, Eur. Phys. J. C **81,** 46 (2021).

[64] Gilberto Colangelo, Martin Hoferichter, and Peter Stoffer, Constraints on the two-pion contribution to hadronic vacuum polarization, Phys. Lett. B **814,** 136073 (2021).

[65] Craig D. Roberts and Anthony G. Williams, Dyson-Schwinger equations and their application to hadronic physics, Prog. Part. Nucl. Phys. **33,** 477 (1994).

[66] Helios Sanchis-Alepuz and Richard Williams, Recent developments in bound-state calculations using the Dyson–Schwinger and Bethe–Salpeter equations, Comput. Phys. Commun. **232,** 1 (2018).

[67] Christian S. Fischer, QCD at finite temperature and chemical potential from Dyson–Schwinger equations, Prog. Part. Nucl. Phys. **105,** 1 (2019).

[68] Ángel S. Miramontes, Hèlios Sanchis Alepuz, and Reinhard Alkofer, Elucidating the effect of intermediate resonances in the quark interaction kernel on the timelike electromagnetic pion form factor, Phys. Rev. D **103,** 116006 (2021).

[69] Muyang Chen, Minghui Ding, Lei Chang, and Craig D. Roberts, Mass-dependence of pseudoscalar meson elastic form factors, Phys. Rev. D **98,** 091505 (2018).

[70] Fei Gao, Lei Chang, Yu-Xin Liu, Craig D. Roberts, and Peter C. Tandy, Exposing strangeness: Projections for kaon electromagnetic form factors, Phys. Rev. D **96,** 034024 (2017).

[71] L. Chang, I. C. Cloët, C. D. Roberts, S. M. Schmidt, and P. C. Tandy, Pion Electromagnetic Form Factor at Spacelike Momenta, Phys. Rev. Lett. **111,** 141802 (2013).

[72] Minghui Ding, Khépani Raya, Daniele Binosi, Lei Chang, Craig D. Roberts, and Sebastian M. Schmidt, Drawing insights from pion parton distributions, Chin. Phys. C **44,** 031002 (2020).

[73] Zhu-Fang Cui, Minghui Ding, Fei Gao, Khépani Raya, Daniele Binosi, Lei Chang, Craig D. Roberts, Jose Rodríguez-Quintero, and Sebastian M. Schmidt, Kaon and pion parton distributions, Eur. Phys. J. C **80,** 1064 (2020).

[74] Chao Shi, Lei Chang, Craig D. Roberts, Sebastian M. Schmidt, Peter C. Tandy, and Hong-Shi Zong, Flavour symmetry breaking in the kaon parton distribution amplitude, Phys. Lett. B **738,** 512 (2014).

[75] Lei Chang, I. C. Cloet, J. J. Cobos-Martinez, C. D. Roberts, S. M. Schmidt, and P. C. Tandy, Imaging Dynamical Chiral Symmetry Breaking: Pion Wave Function on the Light Front, Phys. Rev. Lett. **110,** 132001 (2013).

[76] K. Raya, L. Chang, A. Bashir, J. J. Cobos-Martinez, L. X. Gutiérrez-Guerrero, C. D. Roberts, and P. C. Tandy, Structure of the neutral pion and its electromagnetic transition form factor, Phys. Rev. D **93,** 074017 (2016).

[77] Khepani Raya, Minghui Ding, Adnan Bashir, Lei Chang, and Craig D. Roberts, Partonic structure of neutral pseudoscalars via two photon transition form factors, Phys. Rev. D **95,** 074014 (2017).

[78] Minghui Ding, Khepani Raya, Adnan Bashir, Daniele Binosi, Lei Chang, Muyang Chen, and Craig D. Roberts, $\gamma^*\gamma \to \eta, \eta'$ transition form factors, Phys. Rev. D **99,** 014014 (2019).

[79] Khépani Raya, Adnan Bashir, and Pablo Roig, Contribution of neutral pseudoscalar mesons to a_μ^{HLbL} within a Schwinger-Dyson equations approach to QCD, Phys. Rev. D **101,** 074021 (2020).

[80] Gernot Eichmann, Christian S. Fischer, Esther Weil, and Richard Williams, On the large-Q^2 behavior of the pion transition form factor, Phys. Lett. B **774,** 425 (2017).

[81] Pieter Maris and Peter C. Tandy, The pi, K+, and K0 electromagnetic form-factors, Phys. Rev. C **62,** 055204 (2000).

[82] Ángel S. Miramontes and Hèlios Sanchis-Alepuz, On the effect of resonances in the quark-photon vertex, Eur. Phys. J. A **55,** 170 (2019).

[83] Si-xue Qin and Craig D. Roberts, Impressions of the continuum bound state problem in QCD, Chin. Phys. Lett. **37,** 121201 (2020).

[84] Daniele Binosi, Lei Chang, Joannis Papavassiliou, Si-Xue Qin, and Craig D. Roberts, Symmetry preserving truncations of the gap and Bethe-Salpeter equations, Phys. Rev. D **93,** 096010 (2016).

[85] Gernot Eichmann, Helios Sanchis-Alepuz, Richard Williams, Reinhard Alkofer, and Christian S. Fischer, Baryons as relativistic three-quark bound states, Prog. Part. Nucl. Phys. **91,** 1 (2016).

[86] Markus Q. Huber, Nonperturbative properties of Yang–Mills theories, Phys. Rep. **879,** 1 (2020).

[87] Luis Albino, Adnan Bashir, Bruno El-Bennich, Eduardo Rojas, Fernando E. Serna, and Roberto Correa da Silveira, The impact of transverse Slavnov-Taylor identities on dynamical chiral symmetry breaking, J. High Energy Phys. 11 (2021) 196.

[88] M. Atif Sultan, Khépani Raya, Faisal Akram, Adnan Bashir, and Bilal Masud, Effect of the quark-gluon vertex on dynamical chiral symmetry breaking, Phys. Rev. D **103,** 054036 (2021).

[89] L. Albino, A. Bashir, L. X. Gutiérrez Guerrero, B. El Bennich, and E. Rojas, Transverse Takahashi identities and their implications for gauge independent dynamical chiral symmetry breaking, Phys. Rev. D **100,** 054028 (2019).

[90] Si-Xue Qin and Craig D. Roberts, Resolving the Bethe–Salpeter Kernel, Chin. Phys. Lett. **38,** 071201 (2021).

[91] Zanbin Xing, Khépani Raya, and Lei Chang, Quark anomalous magnetic moment and its effects on the ρ meson properties, Phys. Rev. D **104,** 054038 (2021).

[92] Si-Xue Qin, Craig D. Roberts, and Sebastian M. Schmidt, Ward–Green–Takahashi identities and the axial-vector vertex, Phys. Lett. B **733,** 202 (2014).

[93] Mandar S. Bhagwat, Lei Chang, Yu-Xin Liu, Craig D. Roberts, and Peter C. Tandy, Flavour symmetry breaking and meson masses, Phys. Rev. C **76,** 045203 (2007).

[94] A. Bender, Craig D. Roberts, and L. Von Smekal, Goldstone theorem and diquark confinement beyond rainbow ladder approximation, Phys. Lett. B **380,** 7 (1996).

[95] Yin-Zhen Xu, Daniele Binosi, Zhu-Fang Cui, Bo-Lin Li, Craig D Roberts, Shu-Sheng Xu, and Hong Shi Zong, Elastic electromagnetic form factors of vector mesons, Phys. Rev. D **100,** 114038 (2019).

[96] Fernando E. Serna, Chen Chen, and Bruno El-Bennich, Interplay of dynamical and explicit chiral symmetry breaking effects on a quark, Phys. Rev. D **99,** 094027 (2019).

[97] Lei Chang, Yu-Bin Liu, Khépani Raya, J. Rodríguez-Quintero, and Yi-Bo Yang, Linking continuum and lattice quark mass functions via an effective charge, Phys. Rev. D **104,** 094509 (2021).

[98] Si-xue Qin, Lei Chang, Yu-xin Liu, Craig D. Roberts, and David J. Wilson, Interaction model for the gap equation, Phys. Rev. C **84,** 042202 (2011).

[99] Gernot Eichmann, Christian S. Fischer, Esther Weil, and Richard Williams, Single pseudoscalar meson pole and pion box contributions to the anomalous magnetic moment of the muon, Phys. Lett. B **797,** 134855 (2019); Erratum, Phys. Lett. B **799,** 135029 (2019).

[100] Pieter Maris and Peter C. Tandy, Electromagnetic transition form-factors of light mesons, Phys. Rev. C **65,** 045211 (2002).

[101] Pieter Maris and Peter C. Tandy, The Quark photon vertex and the pion charge radius, Phys. Rev. C **61,** 045202 (2000).

[102] Christian S. Fischer, Dominik Nickel, and Jochen Wambach, Hadronic unquenching effects in the quark propagator, Phys. Rev. D **76,** 094009 (2007).

[103] Christian S. Fischer, Dominik Nickel, and Richard Williams, On Gribov's supercriticality picture of quark confinement, Eur. Phys. J. C **60,** 47 (2009).

[104] Marc Knecht and Andreas Nyffeler, Hadronic light by light corrections to the muon g-2: The Pion pole contribution, Phys. Rev. D **65,** 073034 (2002).

[105] Robert Delbourgo and Peter C. West, A gauge covariant approximation to quantum electrodynamics, J. Phys. A **10,** 1049 (1977).

[106] H. P. Blok *et al.*, Charged pion form factor between $Q^2 = 0.60$ and 2.45 GeV^2. I. Measurements of the cross section for the ^{1}H$(e, e'\pi^+)n$ reaction, Phys. Rev. C **78,** 045202 (2008).

[107] E. B. Dally *et al.*, Direct Measurement of the Negative Kaon Form-Factor, Phys. Rev. Lett. **45,** 232 (1980).

[108] S. R. Amendolia *et al.*, A measurement of the kaon charge radius, Phys. Lett. B **178,** 435 (1986).

[109] S. R. Amendolia *et al.*, A measurement of the space—like pion electromagnetic form-factor, Nucl. Phys. **B277,** 168 (1986).

[110] T. Hahn, CUBA: A library for multidimensional numerical integration, Comput. Phys. Commun. **168,** 78 (2005).

[111] P. A. Zyla *et al.*, Review of particle physics, Prog. Theor. Exp. Phys. **2020,** 083C01 (2020).

[112] R. A. Williams, C. R. Ji, and S. R. Cotanch, Kinematically accessible vector meson resonance enhancements in $p(K^-, e^+e^-) \wedge, \Sigma^0, \wedge (1405)$, Phys. Rev. C **48,** 1318 (1993).

[113] G. Ramalho and M. T. Peña, $\gamma * NN * (1520)$ form factors in the timelike regime, Phys. Rev. D **95,** 014003 (2017).

[114] Carlos Granados, Stefan Leupold, and Elisabetta Perotti, The electromagnetic Sigma-to-Lambda hyperon transition form factors at low energies, Eur. Phys. J. A **53,** 117 (2017).